Spectral function for finite nuclei in the local-density approximation

D. Van Neck and A.E.L. Dieperink
Kernfysisch Versneller Instituut, Zernikelaan 25, 9747 AA Groningen, The Netherlands

E. Moya de Guerra
Instituto de Estructura de la Materia, Consejo Superior de Investigaciones Cientificas, Serrano 119, 28006 Madrid, Spain
(Received 16 September 1994)

The spectral function for finite nuclei is computed within the framework of the local-density approximation, starting from nuclear matter spectral functions obtained with a realistic nucleon-nucleon interaction. The spectral function is decomposed into a single-particle part and a "correlated" part; the latter is treated in the local-density approximation. As an application momentum distributions, quasiparticle strengths and overlap functions for valence hole states, and the light-cone momentum distribution in finite nuclei are computed.

PACS number(s): 24.10.Cn, 21.60.−n, 21.10.Jx

I. INTRODUCTION

All information on the single-particle structure of nuclei is contained in the spectral function $S(k,E)$, where k and E are the momentum and the removal energy of the nucleon, respectively. This quantity plays a central role in a variety of high-energy nuclear reactions, such as in (inclusive and exclusive) quasifree electron scattering and deep-inelastic lepton scattering on nuclei. With presently available many-body techniques (method of correlated basis functions) it can be computed quite accurately for nuclear matter starting from a realistic nucleon-nucleon interaction [1]. On the other hand, for finite nuclei with $A > 4$ it is much more difficult to calculate the spectral function without making severe approximations.

In this paper we compute the spectral function for finite nuclei in the local-density approximation (LDA). To this end the spectral function is decomposed in terms of a single-particle contribution and a correlation part. The former part, which varies strongly with mass number, is represented by the generalized mean field approximation; the latter which is rather insensitive to the finite size of nuclei is treated in the LDA. As an input the results for the nuclear matter spectral function, computed as a function of the density by Fabrocini *et al.* [2,3], are used. In order to get an idea about the sensitivity to the details of the high-momentum components, we also use as an input a simple parametrization of the momentum distribution in nuclear matter given by Baldo *et al.* [4].

Several applications are considered. First, by integrating over the removal energy, momentum distributions for finite nuclei with closed shells are computed. Next we consider three different aspects of the spectral function: (1) the quasiparticle strength for valence hole states and the radial shape of the overlap functions which have been measured in $(e,e'p)$ reactions in several closed shell nuclei, (2) the distribution of single-particle (SP) strength at large removal energies where there is an important enhancement of the high-momentum components in the spectral function, and (3) finally, the light-cone momentum distribution, which plays a central role in the convolution approach to the EMC effect in deep-inelastic scattering on nuclei is computed.

This paper is organized as follows. In Sec. II the LDA to the spectral function is described; Sec. III deals with various applications; Sec. IV contains a summary and discussion.

II. THE SPECTRAL FUNCTION IN THE LOCAL-DENSITY APPROXIMATION

Usually the spectral function for a finite system is expressed in terms of a (truncated) single-particle basis $S_{\alpha\beta}(E) = \langle 0|c_\alpha^\dagger \delta(E - H + E_0) c_\beta|0\rangle$. Since we are interested in the effects induced by (short-range) nucleon-nucleon correlations on the spectral function, we wish to be independent of the choice and size of the SP basis and use the coordinate representation.

For a finite nucleus the hole spectral function can be expressed as

$$S_A(\mathbf{R},\mathbf{r},E) = \langle 0(A)|c^\dagger(\mathbf{r}_1)\delta(E - \hat{H} + E_{0(A)})c(\mathbf{r}_2)|0(A)\rangle \tag{1}$$

with $\mathbf{R} = \frac{1}{2}(\mathbf{r}_1 + \mathbf{r}_2)$ and $\mathbf{r} = \mathbf{r}_1 - \mathbf{r}_2$.

The spectral function (1) is normalized to the number of particles

$$\int d\mathbf{R} \int_{-\epsilon_{F(A)}}^{+\infty} dE\, S_A(\mathbf{R},\mathbf{r}=0,E) = A. \tag{2}$$

We use the convention $\epsilon_{F(A)} = (E_{0(A+1)} - E_{0(A-1)})/2$ for the Fermi energy in a finite system.

In order to make the connection to nuclear matter, it is useful to introduce the Fourier transform with respect to the relative distance $\mathbf{r}$:

$$S_A(\mathbf{R},\mathbf{k},E) = \frac{1}{(2\pi)^3} \int d\mathbf{r} e^{-i\mathbf{k}\cdot\mathbf{r}} S_A(\mathbf{R},\mathbf{r},E). \tag{3}$$

The rhs of Eq. (3) can be interpreted as the spectral function for a nucleon at position $\mathbf{R}$ with momentum $\mathbf{k}$ [2,3]. In particular the momentum distribution in the ground state of a nucleus with mass A is given by

$$n_A(k) = \int d\mathbf{R} \int_{-\epsilon_{F(A)}}^{+\infty} dE\, S_A(\mathbf{R}, \mathbf{k}, E). \tag{4}$$

For our purpose of making a LDA, it is necessary to decompose the spectral function and momentum distribution into a (generalized) *single-particle* part and a *correlation* part. The reason for this can be seen if one considers the global application of the LDA to the (special) case of the momentum distribution

$$n_A^{\mathrm{GLDA}}(k) = \frac{1}{2\pi^3} \int d\mathbf{R}\, \nu(\rho(R), k), \tag{5}$$

where $\nu(\rho, k)$ is the momentum density for nuclear matter at density ρ and with Fermi momentum $k_F(\rho) = (\frac{3}{2}\pi^2\rho)^{1/3}$. As noted in [5], Eq. (5) is divergent in the limit $k \to 0$. This problem can be circumvented by decomposing the momentum distribution into a *mean-field* part and a *correlation* part generated by dynamical excitations. While the former part can be calculated using modern mean-field theories such as density dependent Hartree-Fock, the latter part can then be approximated by applying the LDA to the correlation part of $\nu(\rho, k)$ only, i.e.,

$$\begin{aligned} n_A(k) = n_A^{\mathrm{MF}}(k) &+ \frac{1}{2\pi^3} \int d\mathbf{R}\, \delta\nu_<(\rho(R), k) \\ &+ \frac{1}{2\pi^3} \int d\mathbf{R}\, \delta\nu_>(\rho(R), k) \end{aligned} \tag{6}$$

with

$$\begin{aligned} n_A^{\mathrm{MF}}(k) &= \frac{1}{(2\pi)^3} \int d\mathbf{R} d\mathbf{r} e^{-i\mathbf{k}\cdot\mathbf{r}} n_A^{\mathrm{MF}}(\mathbf{R}, \mathbf{r}), \\ \delta\nu_<(\rho, k) &= (\nu(\rho, k) - 1)\theta(k_F - k), \\ \delta\nu_>(\rho, k) &= \nu(\rho, k)\theta(k - k_F), \end{aligned} \tag{7}$$

and the mean-field density given by the sum over the occupied orbitals

$$n_A^{\mathrm{MF}}(\mathbf{R}, \mathbf{r}) = \sum_{h=1}^{A} n_h^{\mathrm{MF}}(\mathbf{R}, \mathbf{r}) = \sum_{h=1}^{A} \phi_h^*(\mathbf{r}_1)\phi_h(\mathbf{r}_2). \tag{8}$$

A similar divergence problem, which occurs if the LDA is applied to the full spectral function, can be treated in an analogous way. In this case there are several ways to decompose S in different parts. Let us first consider only the mean-field part of the interaction felt by a nucleon in the nucleus, in which case the spectral function has the simple form

$$S_A^{\mathrm{SP}}(\mathbf{R}, \mathbf{r}, E) = \sum_{h=1}^{A} n_h^{\mathrm{MF}}(\mathbf{R}, \mathbf{r})\delta(E + \epsilon_h). \tag{9}$$

In addition to the hole orbitals appearing in Eqs. (8) and (9), the mean field also defines the normally empty particle orbitals ϕ_p. As for deviations from the mean-field approximation, it is convenient to distinguish the following two dynamical effects of the residual interaction.

(i) Depletion and fragmentation of the hole strength. Nucleon-nucleon correlations lead to both depletion and fragmentation of the single hole strength in Eq. (9). We assume that this depletion and fragmentation of the strength related to the hole orbital h only depend on the single-hole energy, ϵ_h; they are taken equal to the depletion and fragmentation of the spectral function $S_{\mathrm{nm}}(\rho, k, E)$ in nuclear matter at the local density. Consequently the δ function in the single-particle part of the correlated spectral function in Eq. (9) is replaced by the distribution function

$$\delta(E + \epsilon_h) \to S_{\mathrm{nm}}(\rho(R), k(\epsilon_h), E). \tag{10}$$

This ensures a realistic behavior of the strength distribution at large removal energies; it is well known that Lorentzian distributions become inadequate away from the quasiparticle peak and cannot be used for the evaluation of, e.g., mean removal energies. The momentum $k(\epsilon_h) < k_F$ corresponding to ϵ_h is chosen in such a way that the SP energy (relative to the Fermi energy) $\epsilon_{F(A)} - \epsilon_h$ corresponds to the position of the quasihole peak in the nuclear matter spectral function. For the most deeply bound hole orbitals it may happen that the SP energy $\epsilon_{F(A)} - \epsilon_h$ lies above the quasihole spectrum for nuclear matter at small density, so no corresponding momentum $k(\epsilon_h)$ can be found. In this case we assigned momentum $k(\epsilon_h) = 0$ to the hole state. It should be mentioned that the contribution of the most deeply bound orbitals to the spectral function is quite insensitive to the nuclear matter results at small densities, since these orbitals are almost exclusively localized in the large-density (interior) region of the nucleus; e.g., 90% of the $1s1/2$ orbital in ^{16}O lies at densities $\rho/\rho_0 > 0.25$, with $\rho_0 = 0.16\,\mathrm{fm}^{-3}$ the nuclear matter density at equilibrium. The fact that the finite volume of the nucleus imposes discrete energies and bound single-particle wave functions ϕ_h (of well-defined angular momentum) is taken into account by keeping the mean-field density $n_h^{\mathrm{MF}}(\mathbf{R}, \mathbf{r})$ in Eq. (9). The single-particle part is dominated by the mean field, and the k dependence is mainly determined by the hole orbitals.

(ii) Partial occupancy of the normally empty states. The scattering of nucleon-nucleon pairs into states above the Fermi momentum leads to both a depletion of the occupied Fermi sea and to the presence of high-momentum components in the spectral function at large removal energies. Since this effect is expected to depend only weakly on the shape of the orbitals ϕ_p in the finite nucleus, the correlation part of S_A is taken equal to the spectral function in nuclear matter for $k > k_F$ at the local density $\rho(R)$:

$$S_A^{\mathrm{cor}}(\mathbf{R}, \mathbf{k}, E) = \frac{1}{2\pi^3} S_{\mathrm{nm}}(\rho(R), k, E)\theta(k - k_F(R)). \tag{11}$$

We emphasize again that this prescription cannot be extended to the whole spectral function ($k < k_F$), since an integration over $\mathbf{R}$ would lead to a singular result for

the momentum distribution at $k = 0$ [see Eq. (5)]. The separation of the spectral function into a single-particle part and a correlation part is thus quite natural, as the low-momentum part of the spectral function depends crucially on the finiteness of the system.

In summary, we use the following decomposition of the hole spectral function:

$$S_A(\mathbf{R},\mathbf{k},E) = S_A^{\rm SP}(\mathbf{R},\mathbf{k},E) + S_A^{\rm cor}(\mathbf{R},\mathbf{k},E) \quad (12)$$

with

$$S_A^{\rm SP}(\mathbf{R},\mathbf{k},E) = \sum_{h=1}^{A} n_h^{\rm MF}(\mathbf{R},\mathbf{k}) S_{\rm nm}(\rho(R), k(\epsilon_h), E) \quad (13)$$

and $S_A^{\rm cor}(\mathbf{R},\mathbf{k},E)$ given by Eq. (11).

III. APPLICATIONS

A. Nuclear matter input

For the nuclear matter spectral functions we used the results obtained by Fabrocini *et al.* [2,3] for densities $\rho/\rho_0 = 0.25$, 0.5, 0.75, and 1.0. The spectral functions were calculated with correlated basis function (CBF) theory using the Urbana v_{14} nucleon-nucleon (NN) interaction with addition of a three-nucleon force [6]. The calculations involve a variational determination of the correlated ground state and of the $1h$ and $2h1p$ states. Furthermore, perturbative corrections ($2p2h$) to the ground state and ($2h1p$) to the $1h$ states are added.

As noted in Ref. [3] a peculiar feature of the nuclear matter results is that the momentum density does not approach the noninteracting one in the limit of zero density. For example, one finds a rather constant depletion, e.g., $\nu(\rho, k \approx 0) = 0.86$, 0.87, 0.86 for $\rho = \rho_0, \frac{3}{4}\rho_0$, and $\frac{1}{2}\rho_0$, respectively, and similar results for the discontinuity $Z(\rho)$ of $\nu(\rho,k)$ at the Fermi surface. This behavior can be attributed to the fact that in the variational approach the attraction of the NN interaction leads to bound pairs and thus to clustering for low densities. One may argue that this effect is an artifact of the variational approach and is not a realistic density dependence to be used in the LDA for finite nuclei. Therefore, we assumed that $\delta\nu(\rho,k) \to 0$ for $\rho \to 0$ by a smooth extrapolation to zero for densities lower than $\frac{1}{4}\rho_0$. One should note that the final results are quite insensitive to this procedure because the weight of small ρ values is quite small.

To investigate the sensitivity to the nuclear matter input, it is of interest to compare the results with those for simple parametrizations of the nuclear matter momentum distribution as a function of the density. Here we use the parametrization recently given by Baldo *et al.* [4]:

$$\delta\nu(\rho,k) = \begin{cases} -0.21 - 0.13\kappa - 0.19(1-\kappa)\ln(1-\kappa), & \kappa < 1 \\ 0.21 + 0.3\arctan x + 0.82x\ln x, & 1 < \kappa < 2,\ k < 2\ \text{fm}^{-1} \\ \frac{k_F^5}{7.0}\exp(-1.6k), & 2 < k < 4.5\ \text{fm}^{-1}, \end{cases} \quad (14)$$

where $x = (\kappa - 1)/(\kappa^2 + 1)$ and $\kappa = k/k_{\rm F}$. This is an approximate parametrization valid for $k_{\rm F} > 1$ fm^{-1}, in the sense that for $k < 2$ fm^{-1} the result depends on κ only. Since we require that $\delta\nu(\rho,k) \to 0$ for lower densities, we multiplied the above expression for $\delta\nu(\rho,k)$ with k_F^2 for $k_{\rm F} < 1$ fm^{-1}. We also properly renormalized the momentum distribution for all densities considered. The parametrization of Eq. (14) provided a good fit to nuclear matter momentum distributions with $1 < k_F < 1.75$ fm^{-1} calculated to second order in the Brueckner reaction matrix and using a separable representation of the Paris interaction.

In Fig. 1 we compare $\nu(k)$ from the two prescriptions for nuclear matter at two densities. Note that the former has a higher depletion and somewhat stronger correlations.

This is also reflected in Table I, where we list the kinetic energies obtained with the spectral functions of [2] and with the parametrization in [4], as a function of the Fermi momentum in nuclear matter. For the kinetic energies obtained with the spectral functions of [2] we assumed an exponential extrapolation of the momentum distribution for large momenta. We note that the total kinetic energy in the interacting system is roughly twice the free value given by $T_{\rm free} = \frac{3k_F^2}{10m}$.

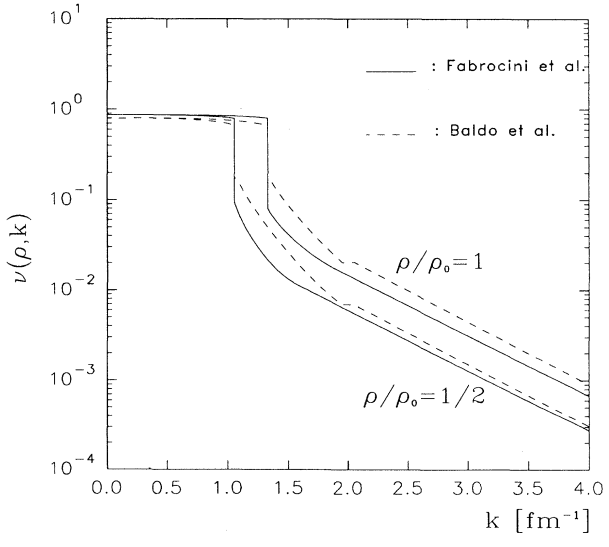

FIG. 1. Nuclear matter momentum distributions (normalized to $\frac{4}{3}\pi k_F^3$) at densities $\rho/\rho_0 = 0.5$ and 1, according to the spectral function of Fabrocini *et al.* [2,3] (solid line) and with the parametrization of Baldo *et al.* (dashed line).

TABLE I. Kinetic energy [MeV] per particle as a function of Fermi momentum in nuclear matter, calculated with the momentum density from Baldo *et al.* [4], and from Fabrocini *et al.* [2,3].

k_F (fm^{-1})	1.13	1.23	1.33
$T_{\rm free}$	15.88	18.82	22.00
Baldo	37.62	42.93	48.31
Fabrocini	33.25	36.99	40.77

B. Momentum distributions in finite nuclei

The momentum distributions for finite nuclei are computed by integrating Eq. (12) over R and E,

$$n_A(k) = n_A^{\rm MF}(k) + \int d\mathbf{R} \sum_h n_h^{\rm MF}(\mathbf{R},\mathbf{k}) \delta\nu_<(\rho(R), k(\epsilon_h)) + \frac{1}{2\pi^3} \int d\mathbf{R} \delta\nu_>(\rho(R), k), \quad (15)$$

for the spherical closed-shell nuclei with A =16, 40, 48, 90, and 208. We checked that the normalization (2) was in all cases fulfilled to better than 1%. The mean-field densities were taken from [7]. For comparison we also used the more conventional form of the LDA of Eq. (6) for the momentum density. The two expressions [Eq. (6) and Eq. (15)] differ in the second term, which represents the depletion of the mean-field momentum distribution at small momenta. In Fig. 2 the resulting momentum densities are compared for ^{16}O and ^{208}Pb. As expected, the high-momentum components ($k > 1.6\,\mathrm{fm}^{-1}$) are identical for both cases. In the intermediate range ($1\,\mathrm{fm}^{-1} < k < 1.6\,\mathrm{fm}^{-1}$), the conventional LDA gives rise to a kink in the momentum distribution. The kink is due to the second term in Eq. (6), which (with $k_{F_{\rm max}}$ the Fermi momentum corresponding to the largest density in the nucleus) has a very steep behavior for $k \lesssim k_{F_{\rm max}}$ and is strictly zero for $k > k_{F_{\rm max}}$. This unphysical feature is removed in the present approach, since the second term in Eq. (15) has a smooth behavior for all k. The present treatment also predicts for ^{16}O somewhat larger $n_A(k)$ for $k \approx 0$ than the conventional LDA, because Eq. (15) takes into account that the reduction of the mean-field distribution for $k \approx 0$ comes only from the depletion of the $1s1/2$ ($l = 0$) orbitals, which are deeply bound and therefore less depleted than the $1p$ orbitals. The conventional LDA, on the other hand, can only take into account an average depletion. For ^{16}O we also included in Fig. 2 the result of a variational Monte Carlo calculation by Pieper *et al.* [8]. As was noted in [3], there is good agreement up to $k = 2\,\mathrm{fm}^{-1}$ between the LDA and the VMC approach. For $k > 2\,\mathrm{fm}^{-1}$ the difference can probably be ascribed to the fact that the VMC calculation was carried out using the Argonne NN interaction, which has a stronger tensor force than the Urbana interaction [8].

In Fig. 3 the LDA result for the A dependence of the momentum density is shown. Although with increasing A there is a clear tendency towards the nuclear matter momentum density, finite-size effects are seen to remain important (even for ^{208}Pb), especially at small k.

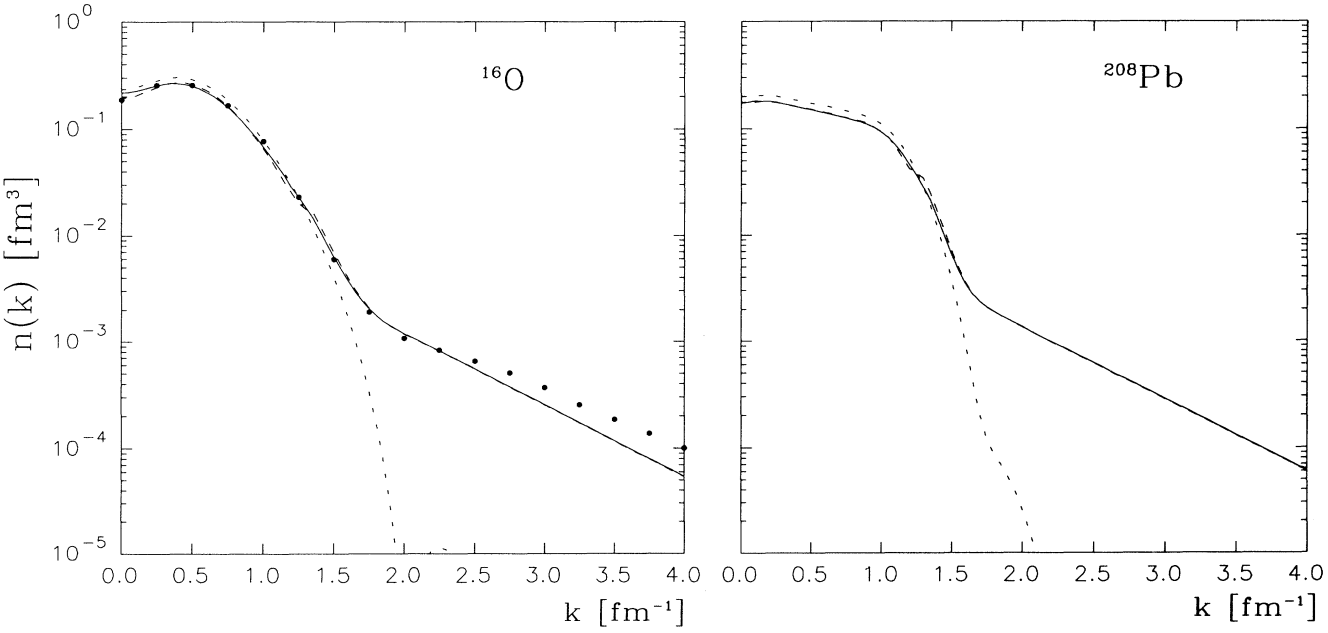

FIG. 2. Momentum density (normalized to unity) in ^{16}O and ^{208}Pb. Short-dashed line: mean-field result. Solid line: present LDA treatment. Long-dashed line: conventional LDA. The dots in the ^{16}O plot were taken from [8].

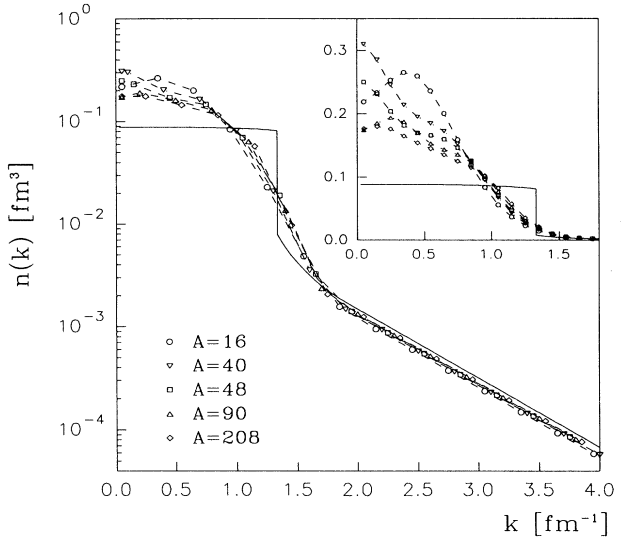

FIG. 3. Momentum density (normalized to unity) for finite nuclei (dashed lines) and nuclear matter at equilbrium density (full line), calculated in the present LDA treatment, with the nuclear matter input taken from [2,3].

The resulting A dependence of the kinetic energy T, $\Delta T = T - T_{\rm MF}$, and the mean removal energy $\langle E\rangle$ are given in Table II. It is seen that both the MF and the correlation part of the kinetic energy amount to approximately 17 MeV, and increase with A. The difference between ΔT in the present approach and in the conventional LDA is small (at most 3%), whereas the parametrization of the nuclear matter momentum density by Baldo *et al.* leads also in finite nuclei to sizably larger ΔT. The mean removal energies $\langle E\rangle$ in Table II were calculated using the mean-field (9) and correlated spectral function (12), and have been corrected for the mean-field rearrangement energy. The inclusion of nucleon-nucleon correlations increases $\langle E\rangle$, from 33 MeV in the mean-field approximation to about 55 MeV. Note that the effects of the Coulomb interaction and the proton-neutron asymmetry are only taken into account via the mean-field single-particle energies. For completeness we have also compared in Table II the experimental binding energies per particle E_A/A with the binding energies following from the Koltun sum rule

$$E_A/A = \frac{1}{2}\left(\frac{A-2}{A-1}T - \langle E\rangle\right), \tag{16}$$

which is valid if only two-body forces are present. We find about 2.4 MeV too much binding. This discrepancy is not too worrisome since we neglected the effect of three-body forces, and (part of) the Coulomb interaction and proton-neutron asymmetry effects.

TABLE II. The A dependence of kinetic and mean removal energies [MeV] per particle. $T^{\rm MF}$ and $\langle E\rangle^{\rm MF}$ refer to the mean-field approximation. $\Delta T^{\rm a}$ and $\Delta T^{\rm b}$ were calculated with the nuclear matter input from Fabrocini *et al.* [2,3], using the present model for the spectral function and the conventional LDA, respectively. For $\Delta T^{\rm c}$ the nuclear matter input from Baldo *et al.* [4] was used, in the conventional LDA. The mean removal energy $\langle E\rangle$ was calculated with the present LDA for the spectral function and includes the mean-field rearrangement energy. E_A/A is the binding energy per particle, calculated using the Koltun sumrule with $\langle E\rangle$ and $T^{\rm a}$.

A	16	40	48	90	208
$T^{\rm MF}$	15.4	16.5	17.7	17.9	18.6
$\Delta T^{\rm a}$	16.3	16.9	17.0	17.3	17.5
$\Delta T^{\rm b}$	15.8	16.5	16.7	17.0	17.3
$\Delta T^{\rm c}$	18.5	20.1	20.7	21.4	22.2
$\langle E\rangle^{\rm MF}$	30.4	33.2	34.8	35.1	34.2
$\langle E\rangle$	50.4	54.0	55.9	56.5	56.6
E_A/A	−10.6	−11.0	−11.1	−11.0	−10.5
E_A/A(expt.)	−8.0	−48.6	−8.7	−8.7	−7.9

[a]See caption.
[b]See caption.
[c]See caption.

C. Spectroscopic factor and radial shape of the quasihole wave functions

1. The LDA approach

Of special interest is the spectral function for the least bound orbitals just below the Fermi energy. For values of the removal energy near the Fermi energy ϵ_F the nuclear matter spectral function vanishes except for momenta slightly below k_F. As a consequence the correlation part $S_A^{\rm cor}$ in Eq. (11) vanishes and the spectral function in LDA can be expressed as

$$S_A(\mathbf{R}, E \approx \epsilon_{F(A)}) = \sum_h \phi_h^*(\mathbf{R})\phi_h(\mathbf{R})Z(\rho(R))\delta(E+\epsilon_h). \tag{17}$$

By comparing Eq. (17) with the general form of the spectral function for the top shells in the $(A-1)$ nucleus

$$S_A(\mathbf{R}, E) = \sum_h |\langle\psi_h^{A-1}|c^\dagger(\mathbf{R})|\psi_A\rangle|^2\delta(E+\epsilon_h) = \sum_h |\psi_h(\mathbf{R})|^2\delta(E+\epsilon_h),$$

one sees that in the LDA the overlap functions $\psi_h(R)$ for the low-lying quasiparticle states can be expressed as

$$\psi_h^{\rm LDA}(\mathbf{R}) = \sqrt{Z(\rho(R))}\phi_h(\mathbf{R}). \tag{18}$$

This result (18) has the correct asymptotic behavior of the overlap function, which is determined by the separation energy of each orbital [9]. It has also been noted that for the case of droplets of ^{3}He atoms, Eq. (18) indeed provides a good approximation to the exact overlap functions [10].

Recent $(e,e'p)$ and (γ,p) experiments (after correction for MEC) have probed the spectral function for the top shells at large missing momenta. Therefore it is of inter-

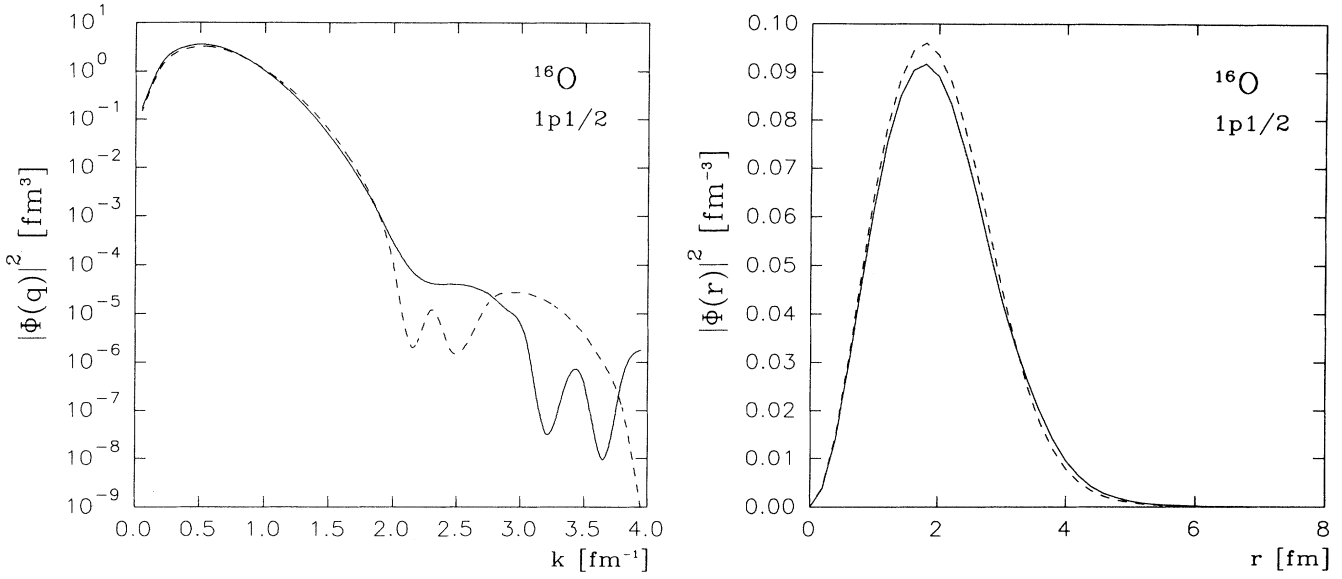

FIG. 4. Overlap function (normalized to unity) for the ^{16}O-1p1/2 state in r space and q space. Dashed line: mean-field approximation. Solid line: including correlations in the LDA according to Eq. (18).

est to examine to what extent the overlap functions for valence hole states are affected by high-momentum components due to short-range NN interactions. One sees from Eq. (18) that in the LDA the only modification of the mean-field wave function in coordinate space can be expressed in terms of a modulation with a density dependent factor that reduces the SP strength.

As a typical example, Fig. 4 shows that the net effect on the radial shape of the $1p_{1/2}$ overlap function in ^{16}O is a slight depletion of the interior and an enhancement of the surface and tail region. In momentum space this leads to only small global deviations from a typical mean-field wave function. This is in agreement with results obtained by Müther and Dickhoff [12,13], who computed the overlap function for the $1p_{1/2}$ orbital in ^{16}O using Green function perturbation theory with a G matrix interaction derived from a realistic NN interaction.

The spectroscopic strength of a quasiparticle state h is in this approach given by

$$Z^{\mathrm{LDA}} = \int d\mathbf{R} Z(\rho(R))|\phi_h(\mathbf{R})|^2. \tag{19}$$

From Fig. 5 one sees that in the LDA the spectroscopic factors (averaged over the valence hole states) decrease slowly with increasing A. This is related to the increase of the mean density with A. In comparison, the data of Ref. [11] also show little A dependence, but the experimental spectroscopic factors are about 0.1 smaller than the LDA prediction.

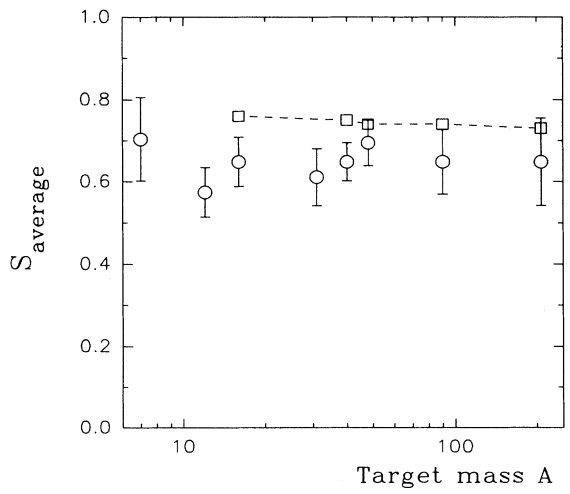

FIG. 5. Average spectroscopic factor for the valence hole states, as a function of mass number. The LDA prediction of the present work (squares) is compared with data (circles) taken from a compilation of $(e, e'p)$ measurements in [11].

2. *Inclusion of surface effects*

One effect not taken into account in a LDA treatment of correlations is the occurrence of surface degrees of freedom in finite nuclei. In particular, collective low-lying excitations in the core nucleus (surface vibrations) are known to couple strongly to the valence SP states, and may affect the shape of the radial overlap function. Namely, the valence hole state in the residual $(A-1)$ nucleus has one-phonon–one-hole components which can have a nonvanishing single-particle overlap with two-phonon components in the ground state of the target nucleus. This leads to admixtures in the overlap function of

SP states which, in contrast to the hole mean-field wave functions, do have sizable components in the momentum range $1.5 < k < 2.5\,\mathrm{fm}^{-1}$.

Following Refs. [15,16] we have included the effect of surface vibrations on the overlap functions in ^{208}Pb through the energy dependence of the mean field. In general both the nonlocality and the genuine energy dependence can be included by the introduction of a total effective mass $m^*(R)$ as the product of a k mass (m_k) and an E mass (m_E)

$$\frac{m^*(R)}{m} = \frac{m_k(R)}{m}\frac{m_E(R)}{m}. \tag{20}$$

Since we assume that the nonlocality (giving rise to m_k) is already included in the Skyrme Hartree-Fock wave functions and that all volume contributions to m_E are already incorporated in the LDA, we only take into account explicitly the surface peaked E mass $m_E(R)/m = (1 + \beta_S dg/dR)$. Here the central part of the mean-field potential $g(R)$ and the parameter β_S, which reflects the coupling strength of the surface modes to the SP states, were taken from [16]. We find that he resulting overlap function $\psi_h^{\mathrm{SV}}(\mathbf{R})$, which includes the effect of surface vibrations, can in good approximation be expressed by an extra modulation factor in Eq. (18)

$$\psi_h^{\mathrm{SV}}(\mathbf{R}) \approx \sqrt{\frac{m_E(R)}{m}}\sqrt{Z(\rho(R))}\phi_h(\mathbf{R}). \tag{21}$$

We have checked, e.g., that for the valence proton SP states in ^{208}Pb the quasiparticle wave functions in [16] are well approximated by the standard Woods-Saxon wave functions multiplied by the effective mass according to (21), although the surface peaking is somewhat overestimated. We note that this prescription was also proposed in Ref. [14].

Figure 6 shows that in momentum space the momentum distributions generated by Eq. (21) are enhanced compared to overlap functions without surface effects, by a factor of 10–100 for momenta in the range $1.5 < k < 2.5$ fm^{-1}. There is indeed recent evidence from an $(e, e'p)$ experiment on ^{208}Pb [14] for a systematic enhancement of the momentum distribution in this range, as compared to mean-field valence hole wave functions. However, in a detailed analysis of the experimental data it should be taken into account that the inclusion of surface effects through a surface-peaked modulation factor changes, e.g., the rms radius of the overlap function, as well as the momentum distribution at smaller momenta.

The extra reduction Z^{SV} of the quasiparticle strength that results from the coupling to surface vibrations can be calculated from the expectation value of $[m_E(R)/m]^{-1}$ with respect to the overlap function ψ_h^{SV}. For the total quasiparticle strength $Z = Z^{\mathrm{SV}}Z^{\mathrm{LDA}}$, we obtain an average of $Z = 0.50$ for the valence hole shells in ^{208}Pb. This result is similar to the one obtained in [17], but is 0.15 lower than the data in [11]. This is probably due to double counting when adding the surface effects to the nuclear matter results.

D. Global distribution of single-particle strength

The energy distribution of total proton hole strength

$$S_A(E) = \int d\mathbf{k} S_A(k, E) \tag{22}$$

is shown in Fig. 7 for ^{208}Pb, split in SP and correlation parts. The SP part is dominant up to 50 MeV removal energy. It represents the quasihole strength corresponding to knockout from the various proton hole shells. Beyond the energy region of the quasihole excitations the SP part of the strength dies out quickly, and the correlation part of the strength, which extends to very high

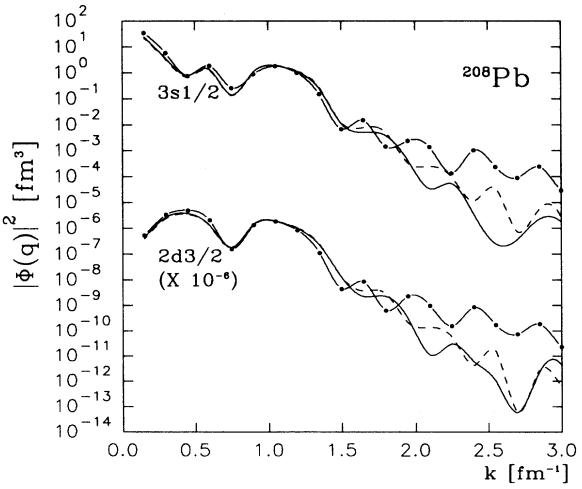

FIG. 6. Overlap function (normalized to unity) in q space for valence proton hole states in ^{208}Pb. Short-dashed line: mean-field approximation. Solid line: including correlations in the LDA according to Eq. (18). Solid line with dots: including additional surface effects according to Eq. (21).

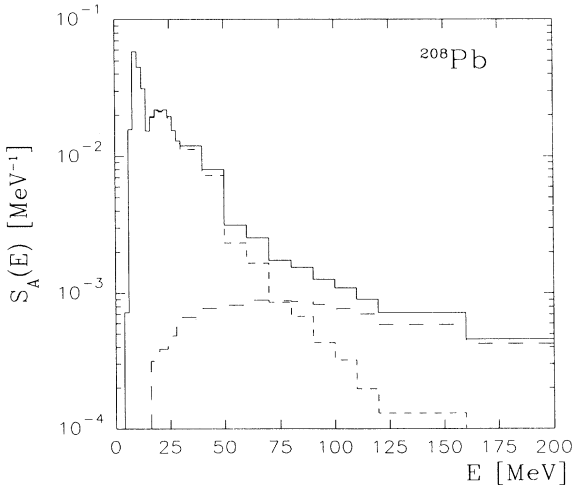

FIG. 7. Proton spectral function for ^{208}Pb, integrated over all momenta, as a function of removal energy. Short-dashed line: single-particle part. Long-dashed line: correlation part. Solid line: total.

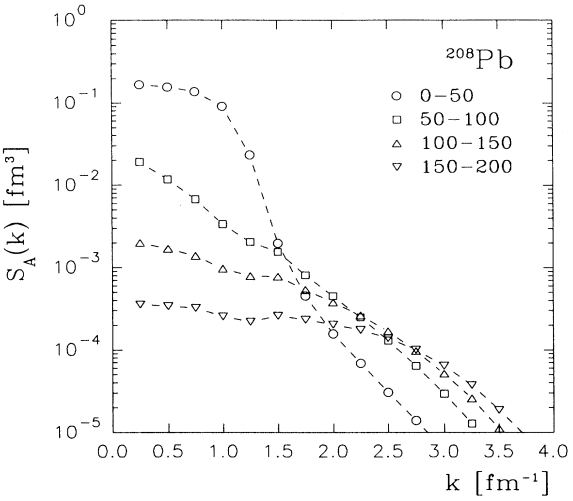

FIG. 8. Proton spectral function for ^{208}Pb, integrated over various regions (0–50, 50–100, 100–150, and 150–200 MeV) of removal energy, as a function of momentum.

removal energies, becomes dominant.

Also of interest is the difference in the momentum distribution between small and large values of the removal energy. Figure 8 clearly illustrates that high-momentum components are correlated with large removal energies, as was also pointed out in [12,13]. Qualitatively this is easily understood, since in order to remove a nucleon with high-momentum in the ground state one has to break a correlated pair. The remaining nucleon in the pair has roughly opposite momentum, its kinetic energy leading to high excitation energies in the residual system.

Comparing with the results quoted in [12,13] it appears that our LDA study predicts a larger amount of high-momentum components, e.g., when integrating the ^{16}O spectral function up to 100 MeV removal energy we find at $k = 2.5$ fm^{-1} about 1.2×10^{-4} fm^3, to be compared with 3.2×10^{-5} fm^3 in [13]. A similar observation holds for the total momentum distribution. A more extensive comparison should be made in order to determine whether these discrepancies arise from differences in the interaction or from shortcomings in either the LDA or in the perturbation scheme used in [12,13].

E. Light-cone momentum distribution

The light-cone momentum distribution plays a central role in the description of high-energy reactions on nuclear targets, such as deep-inelastic scattering. For example, in the simple convolution approach (use of the impulse approximation, and neglecting off-shell effects) to the EMC effect the structure function $F_2^A(x)$ for the A-body target can be expressed as [18]

$$F_2^A(x) = \int_x^\infty dy f_A(y) F_2^N(x/y),$$

where the nuclear structure information is contained in the light-cone momentum distribution

$$f_A(y) = \int dE d^3k S_A(k,E) y \delta\left(y - \frac{k^0 + k^3}{m}\right), \quad (23)$$

where the factor y represents the flux factor. For values of $x < 0.6$ one does not need the full spectral function $S_A(k,E)$, and it is sufficient to expand $F_2^N(x/y)$ around $y = 1$

$$F_2(x/y) = F_2(x) - (y-1)xF_2'(x) + \frac{1}{2}(y-1)^2[2xF_2'(x) + x^2F_2''(x)], \quad (24)$$

and therefore only the lowest moments of $f(y)$ are needed. The lowest moments of $f(y)$ (up to order $\frac{\epsilon^2}{m^2}$) can easily be expressed in terms of T and $\langle E \rangle$

$$\langle y-1 \rangle = \frac{\langle E \rangle + \frac{2}{3}T}{m}, \quad \langle (1-y)^2 \rangle = \frac{2T}{3m}$$

with the result

$$F_2^A(x)/A = F_2^N(x) - \frac{\langle E \rangle}{M} x F_2^{N'}(x) + \frac{T}{3M} x^2 F_2^{N''}(x).$$

In the earlier analysis of the EMC effect for finite nuclei mostly the MF result has been used for $\langle E \rangle$ and T [19], which can explain only 30% of the observed reduction at intermediate x. The inclusion of correlations enhances the effect in the ratio $R_A(x) = F_2^A(x)/AF_2^N(x)$ by about a factor 2, but still cannot fully explain the observed EMC ratio as a function of x [20].

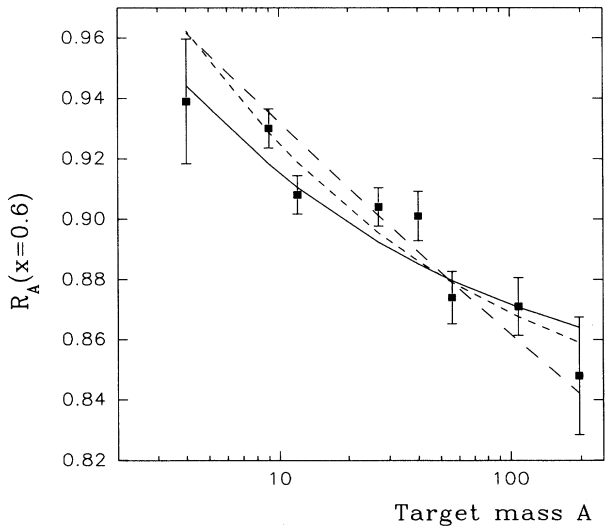

FIG. 9. Mass dependence of the EMC ratio $R_A(x)$, for $x = 0.6$. The SLAC data and best power law fit (long-dashed line) were taken from [21]. Short-dashed line: best fit with the parametrization in terms of a volume and surface contribution (see text). Solid line: LDA prediction for this parametrization.

It is also of interest to examine whether the mass dependence predicted by the convolution method agrees with the observed one. To this end it is convenient to parametrize the A dependence of T and $\langle E \rangle$ in terms of a "volume" and a "surface" term, i.e., $T = T_{\rm vol} - T_{\rm surf} A^{-1/3}$, and similarly for $\langle E \rangle$, hence $R_A(x) = c_1(x) + c_2(x) A^{-1/3}$. As an example, using the best fit values to the LDA results for $T_{\rm vol}$ (=39.38 MeV) and $T_{\rm surf}$ (=18.87 MeV), and using the Koltun sum rule for the mean removal energies, one finds for $x = 0.60$ that $R_A(x) = 0.83 + 0.18 A^{-1/3}$.

Recently a new analysis of the A dependence of deep-inelastic electron scattering at SLAC was presented [21]. In that analysis the EMC ratio for the range of A considered ($2 < A < 197$) was parametrized as a power law: $R_A(x) = C(x) A^{\alpha(x)}$ with $C(x) \approx 1.0$; e.g., at $x = 0.60$ the best fit is obtained for $\alpha(x) = -0.0346 \pm 0.002$. We note that this parametrization has a rather unphysical limit for $A \to \infty$. If we use the more physical parametrization above we obtain $c_1 = 0.82, c_2 = 0.23$, which gives an equally good fit to the data (see Fig. 9) and moreover is in good agreement with our prediction. This indicates that the observed A dependence of the EMC effect is consistent with a purely single nucleon effect. On the other hand if two-body effects would be important a more general mass dependence would be expected.

IV. SUMMARY AND CONCLUSIONS

In this paper we have proposed a method to obtain the single-nucleon spectral function for finite nuclei from that of nuclear matter by applying the local density approximation. Recently a similar method for the construction of the spectral function in finite nuclei was proposed [2] (with the same nuclear matter input) and applied to inclusive electron scattering at large q. The decomposition of the spectral function in [2] is different from ours; e.g., at the variational level the SP part only contains the direct g.s.$\to 1h$ contributions, whereas the g.s.$\to 2h1p$ background contributions are part of the correlation part for both $k < k_F$ and $k > k_F$. On the other hand, in our approach the correlation part contains the full nuclear matter spectral function only for $k > k_F$, whereas the background contribution for $k < k_F$ is incorporated in the generalized single-particle part. However, the resulting momentum distributions for ^{16}O from [2] and from the present work are almost identical.

A point of uncertainty in the LDA treatment of nuclear correlations is the extrapolation of the nuclear matter spectral functions in the limit of zero density, but this is expected to be of little influence on the final results.

We find that correlations lead to an appreciable depletion of quasiparticle strength Z in nuclei; in r space the valence overlap orbital is somewhat more reduced in the interior than in the exterior region, but we find that the momentum distribution of the valence orbit overlap is hardly affected. This agrees with the conclusion in Ref. [12]. However, surface effects may lead, for intermediate momenta, to a considerable enhancement of the momentum distribution for valence hole states.

ACKNOWLEDGMENTS

We would like to thank I. Sick, O. Benhar, and A. Fabrocini for making available to us the results of their calculations of nuclear matter spectral functions at various densities. This work has been supported in part by DGICYT (Spain) under Contract No. PB92/0021-C02-01. This work is part of the research program of the foundation for Fundamental Research of Matter (FOM), which is financially supported by the Netherlands Organisation for Advancement of Pure Research (NWO).

[1] O. Benhar, A. Fabrocini, and S. Fantoni, Nucl. Phys. **A505**, 267 (1989).
[2] I. Sick, S. Fantoni, A. Fabrocini, and O. Benhar, Phys. Lett. B **323**, 267 (1994).
[3] O. Benhar, A. Fabrocini, S. Fantoni, and I. Sick, Report No. SISSA 20/94/CM/MB, 1994.
[4] M. Baldo, I. Bombaci, G. Giansiracusa, U. Lombardo, C. Mahaux, and R. Sartor, Phys. Rev. C **41**, 1748 (1990).
[5] S. Stringari, M. Traini, and O. Bohigas, Nucl. Phys. **A516**, 33 (1990).
[6] I.E. Lagaris and V.R. Pandharipande, Nucl. Phys. **A359**, 331 (1981).
[7] M. Casas, J. Martorell, and E. Moya de Guerra, Phys. Lett. **167B**, 263 (1986); Nucl. Phys. **A473**, 429 (1987).
[8] S.C. Pieper, R.B. Wiringa, and V.R. Pandharipande, Phys. Rev. C **46**, 1741 (1992).
[9] D. Van Neck, M. Waroquier, and K. Heyde, Phys. Lett. B **314**, 255 (1993).
[10] D.S. Lewart, V.R. Pandharipande, and S.C. Pieper, Phys. Rev. B **37**, 4950 (1988).
[11] Nikhef Annual Report 68, Nikhef, Amsterdam (1991).
[12] H. Müther and W.H. Dickhoff, Phys. Rev. C **49**, R17 (1994).
[13] H. Müther, A. Polls, and W.H. Dickhoff, Report No. nucl-th@xxx.lanl.gov:9411005, 1994.
[14] I. Bobeldijk *et al.*, Nikhef report (1994)
[15] C. Mahaux and R. Sartor, Adv. Nucl. Phys. **20**, 1 (1991).
[16] Z.Y. Ma and J. Wambach, Phys. Lett. B **256**, 1 (1991).
[17] O. Benhar, A. Fabrocini, and S. Fantoni, Phys. Rev. **41**, R24 (1990).
[18] L.L. Frankfurt and M.I. Strikman, Phys. Lett. B **183**, 254 (1987); S.A. Kulagin, Nucl. Phys. **A500**, 653 (1989); S.A. Kulagin, G. Piller, and W. Weise, Phys. Rev. C **50**, 1154 (1994).
[19] R.P. Bickerstaff and A.W. Thomas, J. Phys. G **15**, 1523 (1989).
[20] A.E.L. Dieperink and G.A. Miller, Phys. Rev. C **44**, 866 (1991).